

The effect of center-of-mass motion on photon statistics

Yang Zhang, Jun Zhang, Shao-xiong Wu, Chang-shui Yu*

*School of Physics and Optoelectronic Technology, Dalian University of Technology,
Dalian 116024, China*

Abstract

We analyze the photon statistics of a weakly driven cavity quantum electrodynamics system and discuss the effects of photon blockade and photon-induced tunneling by effectively utilizing instead of avoiding the center-of-mass motion of a two-level atom trapped in the cavity. With the resonant interaction between atom, photon and phonon, it is shown that the bunching and anti-bunching of photons can occur with properly driving frequency. Our study shows the influence of the imperfect cooling of atom on the blockade and provides an attempt to take advantage of the center-of-mass motion.

Keywords: Cavity quantum electrodynamics, photon statistics, center-of-mass motion

1. Introduction

The nonlinear interaction represents a hot research topic in recent years. It can lead to a variety of intriguing nonlinear optical phenomena which are ubiquitous in quantum optics, such as the vortex formation, self-focusing, soliton propagation, optical multi-stability and so on [1, 2]. The nonlinear interaction between photons, light or under the influence of Kerr medium [3, 4] has also been widely used to generate nonclassical field states [5, 6] and in the observation of strict quantum effects. Cavity quantum electrodynamics (CQED), as the light and matter meeting interface, is the most straightforward way to produce the quantum nonlinear dynamics [7, 8]. A lot of strict quantum effects such as optical solitons [9], quantum phase transitions [10, 11], quantum squeezing [12] and optical switching with single

*Corresponding author. Tel: +86 41184706201

Email address: quaninformation@sina.com (Chang-shui Yu)

photon [13] have been demonstrated in CQED systems based on the strong optical nonlinearity.

As a typical nonlinear quantum optical effect, photon blockade shows that the system ‘blocks’ the absorption of a second photon with the same energy. The typical feature of this effect is the photon anti-bunching which is signaled by a rise of $g^{(2)}(\tau)$ with τ increasing from 0 to larger values while $g^{(2)}(0) < g^{(2)}(\tau)$ as discussed in detail in Ref [14]. Recently, quantum blockade schemes have been reported in various physical setups such as superconducting circuit [15, 16], cavity arrays [11, 17–19], quantum dots [20, 21], atomic systems [18, 22, 23], quantum optomechanical setups [24–27], confined cavity polaritons [28], systems with ultrastrong coupling [29] and so on [30–32]. What is more, the strong bunching effect, and its special signature called photon-induced tunnelling, which shows the absorption of the first photon can enhance the absorption of the subsequent photons are also been studied [33, 34]. As to the photon blockade in a cavity, the fundamental mechanism is the anharmonic energy-level structure of the light field when the photon-photon interaction is induced by the nonlinear medium [4, 8, 13, 14, 35–40] or induced by the interaction between the trapped multi-level atom and the multi-mode cavity [41], or is observed in the detuned Jaynes-Cummings (J-C) model [33, 42].

In this paper, we study the photon statistics in the detuned J-C model and the effect of the atomic center-of-mass (COM) motion on the photon statistics. Instead of the multi-level atom and the multi-mode cavity, we require that a single two-level atom trapped in a single mode cavity driven by a weak laser and the atom oscillates at its origin with trap frequency. Thus, the photon-photon interaction is induced by the participation of phonons. It is found that the photon blockade is generated under the resonant interaction among atom, photon and phonon, and both the bunching and anti-bunching of photons strongly depend on the atomic motion. In particular, by comparing the cases with and without atomic center-of-mass motion, we find that the atomic center-of-mass motion can enrich the phenomenon of photon statistics. The advantages: on one hand, are to reveal the influence of the atomic center-of-mass motion on the blockade due to the imperfect cooling and on the other hand, are to provide an attempt to taking advantage of the center-of-mass motion of the trapped atom. This paper is organized as follows. In Sec 2, we analyze the equal-time correlation function of cavity mode and demonstrate the photon statistics of J-C model; In Sec 3 we introduce the atomic center-of-mass motion, and investigate the equal-time correlation two-time correlation function of photons; Finally, the conclusion is given in

Sec 4.

2. Equal-time correlation in the detuned J-C model

A two-level system (ion or an atom) couples to the cavity with frequency ω_a which is driven by an external optical field. The frequency of atomic transition from ground state $|g\rangle$ to excited state $|e\rangle$ with linewidth γ is denoted by ω_e . The related Hamiltonian under the rotating wave approximation can be written as [43]

$$H = \Delta a^\dagger a + \delta \sigma^+ \sigma^- + g(a^\dagger \sigma^- + a \sigma^+) + \Omega (a^\dagger + a), \quad (1)$$

where $\Delta = \omega_a - \omega_L$ is the laser detuning from the cavity mode and $\delta = \omega_e - \omega_L$ is the laser detuning from the atom, in the n-excitation subspace, the eigenstates and the eigenvalues can be easily get [43, 44]

$$|n+\rangle = \sqrt{\frac{1}{2} - \frac{\tilde{\delta}}{2\Delta'}} |n, g\rangle + \sqrt{\frac{1}{2} + \frac{\tilde{\delta}}{2\Delta'}} |n-1, e\rangle, \quad (2)$$

$$|n-\rangle = \sqrt{\frac{1}{2} + \frac{\tilde{\delta}}{2\Delta'}} |n, g\rangle - \sqrt{\frac{1}{2} - \frac{\tilde{\delta}}{2\Delta'}} |n-1, e\rangle, \quad (3)$$

with $\tilde{\delta} = \delta - \Delta$ the detuning in frequency between the two-level transition system and cavity mode and $\Delta' = \sqrt{4ng^2 + \tilde{\delta}^2}$ the energy difference between manifold levels. The eigenvalues are $E_{\pm}^{(n)} = (n - \frac{1}{2})\Delta + \frac{1}{2}\delta \pm \frac{\Delta'}{2}$ ($n \geq 1$). We can easily find that the energy splitting has a nonlinear dependence on n (photon number) and gives rise to the nonlinear optics which contains the photon blockade effect and tunneling phenomenon. We will show this in the following part by a strict treatment.

Fig. 1(a) shows the energy diagram of the system. The energy difference value Δ' which is a not a constant, this anharmonic spacing level can affect the photon statistical distribution, such as the photon blockade and photon-induced tunnelling. To understand the photon statistical situation, we will focus on the photon correlation that characterizes the nonclassical photon statistics in the system. Here, we study the equal-time (namely zero-time-delay) second-order photon-photon correlation function [44]:

$$g^{(2)}(0) = \frac{\langle a^\dagger a^\dagger a a \rangle}{\langle a^\dagger a \rangle^2} = \frac{\sum_n n(n-1)p_n}{(\sum_n n p_n)^2}, \quad (4)$$

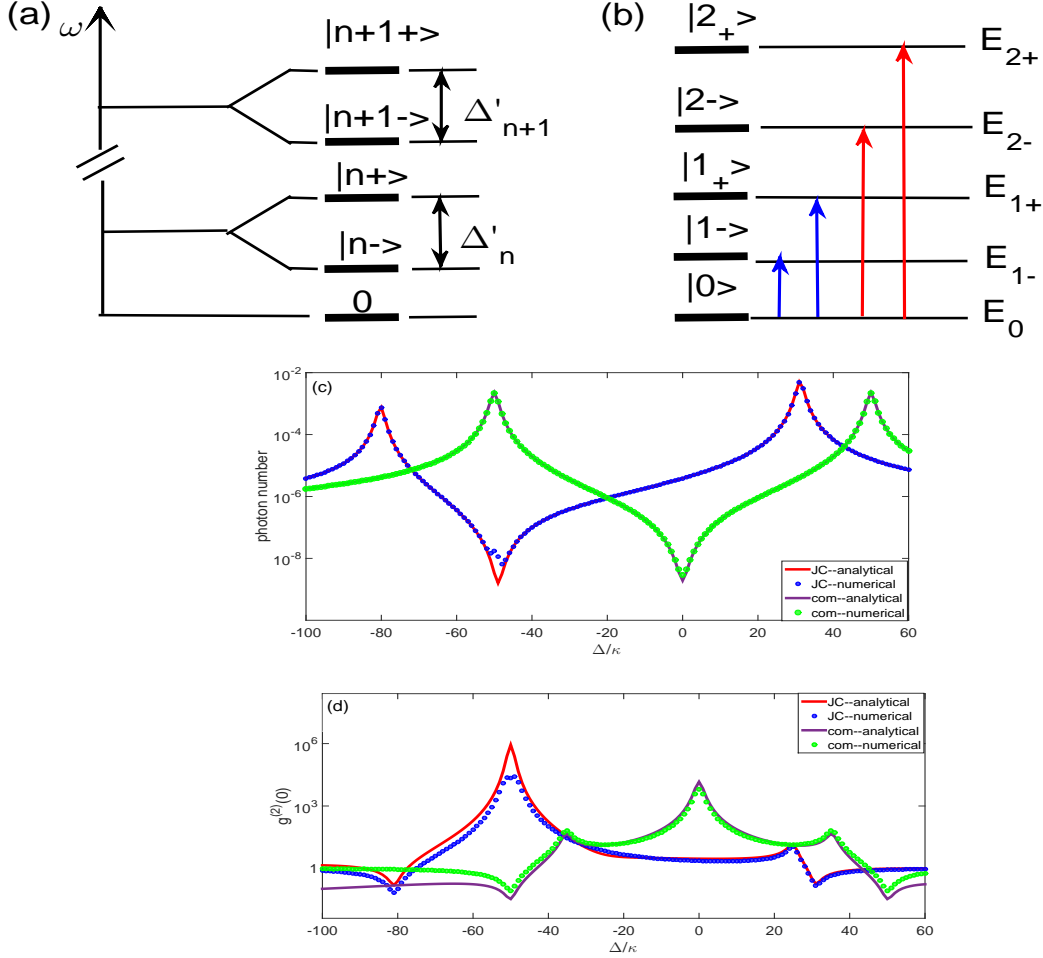


Figure 1: (color online). (a) Diagram for the eigensystem of the Hamiltonian of the coupled cavity-atom system. The anharmonic energy difference between consecutive manifolds is $\Delta' = \sqrt{4ng^2 + \tilde{\delta}}$ which is not constant. (b) The energy diagram with the anharmonic spacing energy under the strong coupling conditions (parameters are chosen as follows). The level shift is caused by the strong coupling. The blue lines indicate the frequency transitions of single photon process for the $|0\rangle \rightarrow |1_{\pm}\rangle$ and red line indicate the two-photon process $|0\rangle \rightarrow |2_{\pm}\rangle$. (c), (d) Mean photon numbers of the cavity and the equal-time second-order function vs. the cavity-laser detuning Δ for the J-C model and atomic center-of-mass motion model. The red and purple curves are approximate analytical solutions of the mean photon number of the J-C model and COM model respectively, while the blue and green dashed curves stand for numerical results based on the solution of the quantum master equation Eq. (13) and Eq. (32). Further explanation of the difference about the two model can be found in the next section. Here all parameters are dimensionless. The parameters are $\gamma/\kappa = 1$, $\Gamma/\kappa = 0.1$, $g/\kappa = 50$, $\delta = \Delta + \tilde{\delta}$, $\Omega/\kappa = 0.1$, $\tilde{\delta}/\kappa = 50$.

where $n = \langle a^\dagger a \rangle$ is the intra-cavity photon number of the cavity mode, p_n represents the probability with n photons. In Eq. (4) the operator is evaluated at the same time. When the photon anti-bunching occurs, the second-order correlation function should fulfill the inequality $g^{(2)}(0) \leq 1$ and the limit $g^{(2)}(0) \rightarrow 0$ corresponds to the perfect photon blockade in which two photons never occupy the cavity at the same time. On the contrary, when $g^{(2)}(0) > 1$, it means photons inside the cavity enhance the resonantly entering probability of subsequent photons [45, 46].

In order to give an intuitive picture, we take an analytical (but approximate) method to calculate the second-order correlation function by employing the wave function amplitude approach. Considering the effects of the leakage of the cavity κ , the spontaneous emission γ of the atom, we phenomenologically add the relevant damping contributions to Eq. (1). Thus the Hamiltonian can be rewritten as $H - i(\kappa a^\dagger a + \gamma \sigma^+ \sigma^-)$. Since we consider the weak driving limit, only few photons can be excited in the cavity. So one can assume that the state of the composite system can be given by [47, 48]

$$|\Psi\rangle = A_{0g}|0, g\rangle + A_{1g}|1, g\rangle + A_{0e}|0, e\rangle + A_{1e}|1, e\rangle + A_{2g}|2, g\rangle. \quad (5)$$

Since the dynamics of the system is governed by Schrödinger equation, using the Hamiltonian and the state $|\Psi\rangle$, we can arrive at the equations about the amplitudes in Eq. (5) as follows.

$$\dot{A}_{1g} = -(\kappa + i\Delta)A_{1g} - i\Omega A_{0g} - igA_{0e} - \sqrt{2}i\Omega A_{2g}, \quad (6a)$$

$$\dot{A}_{01} = -(\gamma + i\delta)A_{01} - igA_{10} - i\Omega A_{11}, \quad (6b)$$

$$\dot{A}_{2g} = -2(\kappa + i\Delta)A_{2g} - \sqrt{2}igA_{1e}, \quad (6c)$$

$$\dot{A}_{1e} = -(\kappa + \gamma + i\delta + i\Delta)A_{1e} - \sqrt{2}igA_{2g} - i\Omega A_{1e}. \quad (6d)$$

Solving Eq. (6) will reveal all the physics. Let the initial state of the system be $|0, g\rangle$. Considering the weak limit of the driving field again, we can get $\bar{A}_{0g} \rightarrow 1$, and the Eq. (6) are closed. Thus, Eq. (6) can be easily solved. In the following, we will only consider the question in the steady-state case. In addition, the steady-state solution of Eq. (6) can be analytically obtained, but the concrete form are quite cumbersome, so we further neglect the high-order terms in Ω (weak driving) and obtain

$$\bar{A}_{1g} = -\frac{i\Omega(\gamma + i\delta)}{g^2 + \tilde{\Delta}}, \quad (7)$$

$$\bar{A}_{0e} = -\frac{g\Omega}{g^2 + \tilde{\Delta}}, \quad (8)$$

$$\bar{A}_{2g} = -\frac{\Omega^2[g^2 - (\gamma + i\delta)^2 - \tilde{\Delta}]}{\sqrt{2}(g^2 + \tilde{\Delta})(g^2 + (\kappa + i\Delta)^2 + \tilde{\Delta})}, \quad (9)$$

$$\bar{A}_{1e} = \frac{ig^2\Omega^2(\gamma + \kappa + i\delta + i\Delta)}{(g^2 + \tilde{\Delta})(g^2 + (\kappa + i\Delta)^2 + \tilde{\Delta})}, \quad (10)$$

with $\tilde{\Delta} = (\gamma + i\delta)(\kappa + i\Delta)$. Thus Eq. (4) can be rewritten as $g^{(2)}(0) = \frac{2p_2}{(p_1 + 2p_2)^2}$, with $p_1 = |\bar{A}_{1g}|^2$, $p_2 = |\bar{A}_{2g}|^2$. In the weak-driving case, we can easily get $p_1 \gg p_2$, then the second-order correlation function

$$g^{(2)}(0) = \frac{|g^2 + \gamma + i\delta|^2 |g^2 - (\gamma + i\delta)^2 - \tilde{\Delta}|^2}{|\gamma + i\delta|^4 |g^2 + (\kappa + i\Delta)^2 + \tilde{\Delta}|^2}, \quad (11)$$

$$\bar{n} = \frac{\Omega^2 |\gamma + i\delta|^2}{|g^2 + \tilde{\Delta}|^2}. \quad (12)$$

In order to show the validity of the above results, we use the Markovian master equation for the model, that is,

$$\dot{\rho} = -i[H, \rho] + \kappa L[a]\rho + \gamma L[\sigma^-]\rho \quad (13)$$

where H is the Hamiltonian given by (1), ρ is the density operator of the whole composite system, and $L[\hat{d}]\rho = 2\hat{d}\rho\hat{d}^\dagger - \hat{d}^\dagger\hat{d}\rho - \rho\hat{d}^\dagger\hat{d}$, ($\hat{d} = \hat{a}, \hat{\sigma}^-$) is the dissipator. In addition, we don't consider the thermal photons for simplicity [45]. Since the steady-state solution is needed for our purpose, we will directly employ a numerical way to solving Eq. (13) for the steady state ρ_s [49]. So the second-order correlation function can be directly obtained by $g^{(2)}(0) = \frac{Tr[\rho_s a^{\dagger 2} a^2]}{[Tr(\rho_s a^\dagger a)]^2}$, and the mean photon number is given by $\bar{n} = Tr(\rho_s a^\dagger a)$.

In what follows, we will employ both the analytical method given by Eq. (11) and the numerical way as Eq. (13) to study the properties of the equal-time correlation function $g^{(2)}(0)$. As is shown in Fig. 1(d), we plot $g^{(2)}(0)$ as a function of the cavity-laser detuning Δ , a different story takes place with resonant condition when the model under the strong coupling region; the detuning $\Delta/\kappa = -50(25)$ corresponds to the red lines in Fig. 1(b), which means the transition $|0\rangle \rightarrow |2_\pm\rangle$ and $g^{(2)}(0) \gg 1$, indicating that the photon

bunching for the cavity. In addition, when $\Delta/\kappa = -50$, it also indicates a quasi-Dark state ($|\hat{d}\rangle \propto g|0, g\rangle - \Omega|0, e\rangle$), which exhibit the strong bunching behavior. At the point of $\Delta/\kappa = -25(1 \pm \sqrt{5})$, $g^{(2)}(0) \ll 1$, indicating the complete photon blockade due to the suppressed two-photon process, corresponds to the blue lines in Fig. 1(b). When $\Delta = 0$, the system does not exhibit the strong bunching behavior as the bare cavity [33], that means the absorption of the first photon can not enhance the absorption of the subsequent photons and the expected photon-induced tunnelling phenomenon disappeared owing the cavity-atom off-resonance.

3. Atomic center-of-mass motion on photon statistics

3.1. The model and equal-time correlation

In this section, we consider the effect of atomic center-of-mass motion on the photon statistics. As shown in Fig. 2(a), a two-level system which is confined by a harmonic potential with the trap frequency ν . In this configuration, the two-level system and cavity are same as before. We suppose that the model is a one-dimensional model and restrict the motion of the atom along the x axis. So the Hamiltonian of this system under the dipole approximation reads [50]

$$H = \omega_a a^\dagger a + \omega_e \sigma^+ \sigma^- + \frac{\hat{p}^2}{2m} + \frac{m\nu^2 \hat{x}^2}{2} + \tilde{g}(k\hat{x})(\sigma^+ a + a^\dagger \sigma^-) + \Omega (a^\dagger e^{-i\omega_L t} + a e^{i\omega_L t}), \quad (14)$$

where \tilde{g} is the position-dependent coupling coefficient, Ω and ω_L are related to the power and frequency of the driving laser, respectively, k denotes the wave number of the field. Note that the third and fourth terms represent the kinetic energy and the harmonic potential respectively, and m represents the mass of the atom. The strength of the interaction of the two-level system with the single mode of cavity is characterized by the coupling operator which is given by [51]

$$\tilde{g}(k\hat{x}) = \tilde{g} \cos(kx \cos \phi + \varphi), \quad (15)$$

where ϕ is the angle between wave vector and axis of the motion, φ accounts for the displacement of the trap center with respect to the origin. For convenience we set $\phi = 0$, $\varphi = \frac{\pi}{2}$, and we also introduce the annihilation and creation operators b and b^\dagger of a quantum of vibrational energy, therefore,

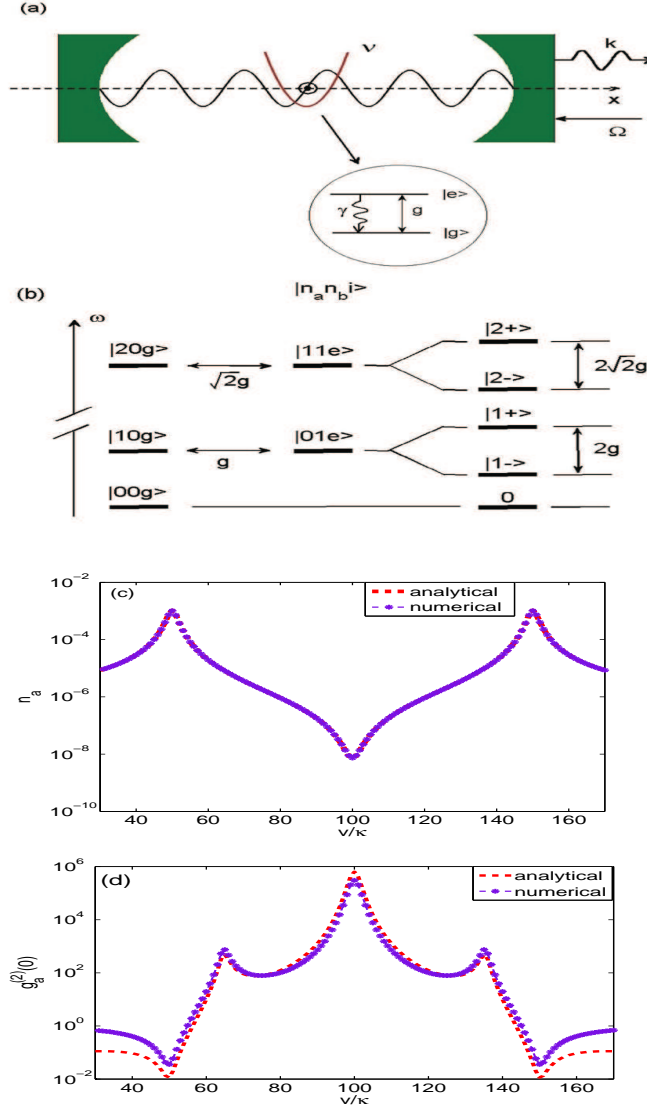


Figure 2: (color online). (a).The center-of-mass motion of a trapped atom under the assumption that the atom is confined within a high-finesse cavity which is pumped by a laser. (b) Diagram of the eigensystem of the Hamiltonian under the resonance condition and level diagram is limited in the subspace spanned by the zero-, one-, and two-photon states. States are labeled by $|n_a, n_b, i\rangle$ denoting the photon numbers of cavity mode, phonon number of mechanical mode and the level of atom. (c),(d): The mean photon numbers of the cavity and the equal-time second-order function $g^{(2)}(0)$ vs. the trap frequency ν respectively. The red curves are approximately analytical solution of Eq. (30) and Eq. (31) while the purple curves are numerical results based on the solution of the quantum master equation Eq. (32). The parameters are chosen the same as Fig. 1.

the position and canonically-conjugated momentum of the atom are given by $\hat{x} = \sqrt{\frac{\hbar}{2mv}}(b + b^\dagger)$, $\hat{p} = i\sqrt{\frac{\hbar mv}{2}}(b^\dagger - b)$. In addition, the third and fourth terms of Hamiltonian (14) can be rewritten as $\hbar v(b^\dagger b + \frac{1}{2})$. Omitting the constants, Hamiltonian (14) becomes (we set $\hbar = 1$ hereafter)

$$H_0 = \omega_a a^\dagger a + \omega_e \sigma^+ \sigma^- + v b^\dagger b + g(a^\dagger \sigma^- + a \sigma^+) (b^\dagger + b) + \Omega (a^\dagger e^{-i\omega_L t} + a e^{i\omega_L t}), \quad (16)$$

with $g = \tilde{g} \frac{\omega_c}{c} \sqrt{\frac{\hbar}{2mv}}$. In the frame rotated at the laser frequency ω_L , we obtain

$$H' = \Delta a^\dagger a + \delta \sigma^+ \sigma^- + v b^\dagger b + g(a^\dagger \sigma^- + a \sigma^+) (b^\dagger + b) + \Omega (a^\dagger + a), \quad (17)$$

Now, we focus on the three-mode resonant interaction in which the cavity and atom exchange a photon by absorbing or emitting a phonon in the mechanical mode. We set $\Delta = \delta + v$ and assume $|\delta| \gg \frac{g}{2}$. In order to study the dynamics of the system, we would like to turn to a rotation framework subject to the transformation $\hat{u}(t) = \exp[-i\hat{R}t]$ with $R = \delta(\sigma^+ \sigma^- - b^\dagger b)$. With the rotating-wave approximation at large detuning δ , the effective Hamiltonian can be given by

$$H_{\text{eff}} = (\delta + v)(a^\dagger a + b^\dagger b) + g(a^\dagger b \sigma^- + a b^\dagger \sigma^+) + \Omega (a^\dagger + a). \quad (18)$$

The second term in the first line of Eq. (18) describes the effective nonlinear coupling proportional to coupling strength g which describes the coherent photon-phonon exchange between the cavity mode and mechanical mode mediated by atomic absorption or emission of a photon. The effective Hamiltonian can be diagonalized in the absence of a driving [47]. The eigenstates distinguished by different numbers of photons and phonons can be expressed as

$$|0\rangle = |0, 0, g\rangle, \quad (19)$$

$$|1_\pm\rangle = \frac{1}{\sqrt{2}}(|1, 0, g\rangle \pm |0, 1, e\rangle), \quad (20)$$

$$|2_\pm\rangle = \frac{1}{\sqrt{2}}(|2, 0, g\rangle \pm |1, 1, e\rangle), \quad (21)$$

where $|n_a, n_b, i\rangle$ ($i = e, g$) are the preferential basis with n_a, n_b denoting the photon number and phonon number, respectively, and $|i\rangle$ ($|g\rangle, |e\rangle$) represents the ground and the excited states of the atom. The low-energy level diagram is sketched in Fig. 2 (b), from which one can see that the states $|1, 0, g\rangle$ and $|0, 1, e\rangle$ are superposed to form two eigenstates $|1_{\pm}\rangle$ splitted by $2g$, and the states $|2, 0, g\rangle$ and $|1, 1, e\rangle$ are superposed to form another two eigenstates $|2_{\pm}\rangle$ splitted by $2\sqrt{2}g$. Intuitively, one can find, from the level diagram, that the resonant absorption of a photon with frequency $\omega_a \pm g$ to reach the state $|1_{\pm}\rangle$ ‘block’ absorb the second photon with the same frequency because of the detuning from the other levels [7, 24, 25, 52].

Using the same approach, we can obtain the following results for the atomic center-of-mass motion system. So we can also assume that the state of the composite system is

$$|\Psi\rangle_{com} = A_{00} |0, 0, g\rangle + A_{10}(|1, 0, g\rangle + A_{01} |0, 1, e\rangle) \quad (22)$$

$$+ A_{11} |1, 1, e\rangle + A_{20} |2, 0, g\rangle \quad (23)$$

The equations about the amplitudes in Eq.(22) as follows.

$$\dot{A}_{10} = -(\kappa + i\Delta)A_{10} - i\Omega A_{00} - igA_{01} - \sqrt{2}i\Omega A_{20}, \quad (24a)$$

$$\dot{A}_{01} = -(\gamma + \Gamma + i\Delta)A_{01} - igA_{10} - i\Omega A_{11}, \quad (24b)$$

$$\dot{A}_{20} = -2(\kappa + i\Delta)A_{20} - \sqrt{2}igA_{11}, \quad (24c)$$

$$\dot{A}_{11} = -(\kappa + \gamma + \Gamma + 2i\Delta)A_{11} - \sqrt{2}igA_{20} - i\Omega A_{11}, \quad (24d)$$

Solving Eq. (24) will reveal all the physics. Let the initial state of the system be $|0, 0, g\rangle$. Considering the weak limit of the driving field again, we can get $\bar{A}_{00} \rightarrow 1$, and obtain the following coupled set of equations for the steady state:

$$-(\kappa + i\Delta)\bar{A}_{10} - i\Omega\bar{A}_{00} - ig\bar{A}_{01} - \sqrt{2}i\Omega\bar{A}_{20} = 0, \quad (25a)$$

$$-(\gamma + \Gamma + i\Delta)\bar{A}_{01} - ig\bar{A}_{10} - i\Omega\bar{A}_{11} = 0, \quad (25b)$$

$$-2(\kappa + i\Delta)\bar{A}_{20} - \sqrt{2}ig\bar{A}_{11} = 0, \quad (25c)$$

$$-(\kappa + \gamma + \Gamma + 2i\Delta)\bar{A}_{11} - \sqrt{2}ig\bar{A}_{20} - i\Omega\bar{A}_{11} = 0, \quad (25d)$$

then we can obtain

$$\bar{A}_{10} = -\frac{i\Omega\tilde{\gamma}}{g^2 + \tilde{\gamma}\tilde{\kappa}}, \quad (26)$$

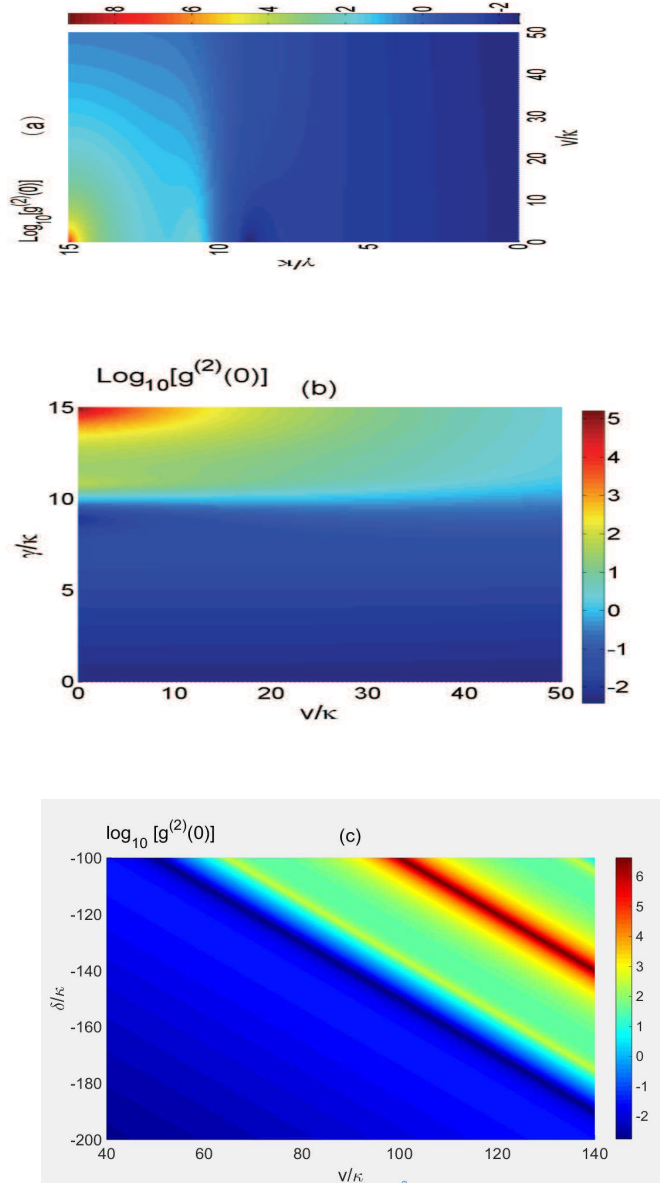


Figure 3: (color online). We plot the $\log_{10} [g^{(2)}(0)]$ as a function of ν and γ for (a) $\Gamma/\kappa = 0.1$ and for (b) $\Gamma/\kappa = 1$. The other parameters are $\delta/\kappa = -50$, $\Omega/\kappa = 0.1$. For (c), we plot the $\log_{10} [g^{(2)}(0)]$ as a function of ν and δ , we take $\gamma/\kappa = 1$, $\Gamma/\kappa = 0.1$, $\Delta = \delta + \nu$, other parameters are the same as (a) and (b).

$$\bar{A}_{01} = -\frac{g\Omega}{g^2 + \tilde{\gamma}\tilde{\kappa}}, \quad (27)$$

$$\bar{A}_{11} = -\frac{ig\tilde{\kappa}\Omega^2}{(g^2 + \tilde{\gamma}\tilde{\kappa})(g^2 + \tilde{\kappa}^2 + \tilde{\gamma}\tilde{\kappa})}, \quad (28)$$

$$\bar{A}_{20} = \frac{g^2\Omega^2}{\sqrt{2}(g^2 + \tilde{\gamma}\tilde{\kappa})(g^2 + \tilde{\kappa}^2 + \tilde{\gamma}\tilde{\kappa})}, \quad (29)$$

where $\tilde{\gamma} = \gamma + \Gamma + i(\delta + \nu)$, $\tilde{\kappa} = \kappa + i(\delta + \nu)$. Thus with $p_1 = |\bar{A}_{10}|^2$, $p_2 = |\bar{A}_{20}|^2$, $p_1 \gg p_2$, the second-order correlation function becomes

$$g_a^{(2)}(0) \approx \frac{2p_2}{p_1^2} = \frac{g^4(g^2 + \tilde{\gamma}^*\tilde{\kappa}^*)(g^2 + \tilde{\gamma}\tilde{\kappa})}{(g^2 + \tilde{\kappa}^{*2} + \tilde{\gamma}^*\tilde{\kappa}^*)(g^2 + \tilde{\kappa}^2 + \tilde{\gamma}\tilde{\kappa})|\tilde{\gamma}|^4}, \quad (30)$$

and the mean photon number is

$$n_a \approx p_1 = \frac{\Omega^2 |\tilde{\gamma}|^2}{(g^2 + \tilde{\gamma}^*\tilde{\kappa}^*)(g^2 + \tilde{\gamma}\tilde{\kappa})}. \quad (31)$$

Meanwhile the master equation is

$$\dot{\rho} = -i[H_{\text{eff}}, \rho] + \kappa L[a]\rho + \gamma L[\sigma^-]\rho + \Gamma L[b]\rho, \quad (32)$$

where H_{eff} is the effective Hamiltonian given by (18), and $L[\hat{d}]\rho = 2\hat{d}\rho\hat{d}^\dagger - \hat{d}^\dagger\hat{d}\rho - \rho\hat{d}^\dagger\hat{d}$, ($\hat{d} = \hat{a}, \hat{b}, \hat{\sigma}^-$) is the dissipator.

In what follows, we will employ both the analytical method given by Eq. (30) and the numerical way as Eq. (32) to study the properties of the equal-time correlation function $g^{(2)}(0)$. As is shown in Fig. 2 (c), we plot $g^{(2)}(0)$ as a function of the trap frequency ν . We find that the photon statistic properties can be controlled by tuning the trap frequency ν . Here, the red curves are plotted using the analytical expression Eq. (30) while the grape curves are based on the numerical solution of Eq. (32). One can see that at $\nu/\kappa = 100$ ($\Delta = 0$), $g^{(2)}(0) \gg 1$ in Fig. 2(d), where the photon satisfy the super-Poissonian distribution. In other words, it indicates that at this point photons occur the bunching behavior. This can be explained that the system presents destructive interference that suppresses the population in $|1, 0, g\rangle$. At this point, the system is driven into a dark state $|dark\rangle \propto g|0, 0, g\rangle - \Omega|0, 1, e\rangle$ which is similar to the electromagnetically induced transparency [53, 54]. In the dark state, $|0, 1, e\rangle$ remains populated, allowing transitions to $|1, 1, e\rangle$ which is strongly coupled to $|2, 0, g\rangle$. The probability

of two photons inside the cavity is resonantly enhanced at this point which corresponds to the peak in the correlation function of $g^{(2)}(0)$. Moreover, we see that at $\nu/\kappa = 100$, the strong bunching regime is accompanied by a suppression of the photon number, the photon-induced tunneling occurs due to the probability of single-photon emission decreases, while the probability for photon pair generation increases. This behavior can also be occurred when $\nu/\kappa = 100 \pm 25\sqrt{2}$, because of the transition $|0\rangle \rightarrow |2_+\rangle$ which is a double photon resonance process. At the frequency $\nu/\kappa = 50$ and 150 , the detuning $\Delta/\kappa = -50$ and 50 correspondingly, the second-order correlation function $g^{(2)}(0) \ll 1$ (i.e., two dips), which shows the anti-bunching and sub-Poissonian distribution. This is consistent with our intuitive analysis given above. That is, the frequency of the driving is resonant with the transition between the state $|0\rangle$ and $|\pm 1\rangle$, which ‘blocks’ the absorption of the second photon due to the detuning.

So far, we have demonstrated the quantum properties with the analytical and numerical methods both in the J-C model and atomic center-of-mass motion model. By comparing the two curves in Fig. 1(d), we find that by introduced phonon degree of freedom, the photon statistics changes as a function of Δ , and photon blockade effect occurs at the different Δ compared with the J-C model which can also be demonstrated by the analytical expressions of second-order correlation function in Eq. (11) and Eq. (30). We can also find that the trap frequency ν leads to an obvious displacement of the maximal peak, whilst it leads to a new bunching peak.

To find the effects of the decay and the detuning on the photon blockade, we plot the logarithm of the correlation function $g^{(2)}(0)$ as a function of γ and ν in Fig. 3. Fig. 3 gives a boundary for different photon distributions such as super-Poissonian and sub-Poissonian distributions. The two regions are distinguished by $\gamma/\kappa \sim 10$ in both Fig. 3(a) and 3(b). These two figures show how the second-order correlation function varies with the decay rates. In particular, one can find that the maximum of $g^{(2)}(0)$ occurs at the top of the figures ($\gamma/\kappa = 15$), but the minimum of $g^{(2)}(0)$ (anti-bunching) is just below $\gamma/\kappa \sim 10$. Between them, there also exists a bunching peak. In Fig. 3 (c), $g^{(2)}(0)$ between bunching and anti-bunching at the frequency ν and detuning δ is illustrated. It is apparent that the photon blockade happens in the region $|\Delta/\kappa| \approx g$, which can be obtained from Eq. (30) by setting the numerator of $g^{(2)}(0)$ vanishes for small dissipations.

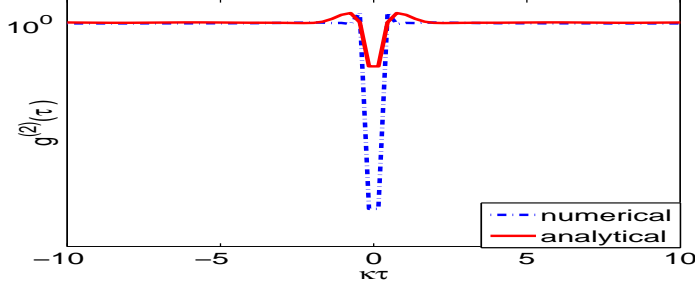


Figure 4: (color online). The evolution of finite time delay correlation function $g^{(2)}(\tau)$ of the atomic center-of-mass motion cavity mode. The red line indicate the analytical expression and the blue dash line denotes the numerical simulation. The parameters are chosen as $g/\kappa = 20$, $\delta/\kappa = -70$, $\Omega/\kappa = 4$, $\gamma/\kappa = 4$, $\Gamma/\kappa = 0.1$, $\nu/\kappa = 50$.

3.2. Delayed coincidence correlation

In addition to the second-order correlation function for equal time discussed in the previous section, some quantum signatures can also be manifested from the photon intensity correlations with the nonzero delay. In this part, we give a discussion of the evolution of the two-time correlation function, which is defined for stationary state by [26, 56]

$$g^{(2)}(\tau) = \frac{\langle a^\dagger(0)a^\dagger(\tau)a(\tau)a(0) \rangle}{\langle a^\dagger a \rangle^2}, \quad (33)$$

Eq. (33) can be rewritten, based on the correlations of classical light intensity I , as $g^{(2)}(\tau) = \frac{\langle I(\tau)I(0) \rangle}{\langle I(0) \rangle^2}$. With the Schwarz inequality for random variables:

$$\langle I_1 I_2 \rangle^2 \leq \langle I_1^2 \rangle \langle I_2^2 \rangle, \quad (34)$$

which means that

$$\langle I(\tau)I(0) \rangle^2 \leq \langle I(\tau)^2 \rangle \langle I(0)^2 \rangle. \quad (35)$$

The inequality is saturated if $\tau = 0$. Thus one can further find that [44, 57]

$$g^{(2)}(\tau) \leq g^{(2)}(0). \quad (36)$$

Similar to the classical inequality, $g^{(2)}(0) > 1$ at zero delay, and violation of the inequality at finite delay is a unique signature of quantum system. Next

we will calculate the delayed second-order correlation function for the cavity mode. The two-time correlation functions can be understood in terms of the five-level model discussed above. For this purpose, we may use the standard method to calculate the two-time correlation function with a conditional state as the initial condition [58]. The unnormalized state after the annihilation of a photon in the cavity is $a|\Psi\rangle = \bar{A}_{10}(|0, 0, g\rangle + \bar{A}_{11}|0, 1, e\rangle + \sqrt{2}\bar{A}_{20}|1, 0, g\rangle$. By solving the Eq. (11)(a)-(d) with this state as the initial condition, one can obtain the time-delayed correlation function as

$$g^{(2)}(\tau) = \frac{|A_{10}(\tau)|^2}{|\bar{A}_{10}|^4}. \quad (37)$$

The positive derivative of the time-delayed correlation function with respect to variable τ represents a nonclassical behavior of the system. Additionally, it is important for the experimental observation of the anti-bunching, since the precise measurement of the equal-time correlation function may be challenging [59]. Both the analytical and numerical results of the two types cavity mode are plotted in Fig. 4. We can observe that according to the system nonlinearity the time-dependent second-order correlation function shows the quantum signature which violates the inequality in Eq. (36) because $g^{(2)}(\tau)$ going beyond their initial value at finite time delay. We note that the behavior of the second-order correlation function in this case is similar to the single-photon diode in the semiconductor microcavities coupled via $\chi(2)$ nonlinearities [60]. This can be attributed to the fact the strong nonlinearity of our system for both the zero and the finite time delay correlation functions.

4. Conclusion

We have studied the photon blockade effect in CQED system weakly driven by a monochromatic laser field, in which an atom is trapped inside. The spirit of this scheme is to effectively take advantage of the atomic center-of-mass motion instead of avoiding it. By the numerical and the approximate analytical expressions of the one-time and two-time second-order correlation function for the cavity photons, we have identified several different processes that can lead to photon-induced tunnelling and photon blockade, our study provides another way on photon control using a atomic center-of-mass motion system. In addition, the trap-frequency dependent blockade effect directly

shows the influence of imperfect cooling, whilst it may induce the other potential applications of atomic center of mass motion in quantum information processing.

Finally, we would like to say that trapped ions or atoms are well suited for this purpose as the quantum technology for controlling their degrees of freedom that is already well developed [62, 63]. The coupling to the cavity has been successfully employed for implementation of a photon-mediated entanglement distribution [62–64] and the cooling the motion of an atom which is trapped by a harmonic trap [51, 65–67]. The combination with the coupling to the field of high-finesse resonators can bring novel perspective for the manipulation of the atomic motion.

Acknowledgement

This work was supported by the National Natural Science Foundation of China, under Grant No.11375036 and 11175033, the Xinghai Scholar Cultivation Plan and the Fundamental Research Funds for the Central Universities under Grant No. DUT15LK35.

References

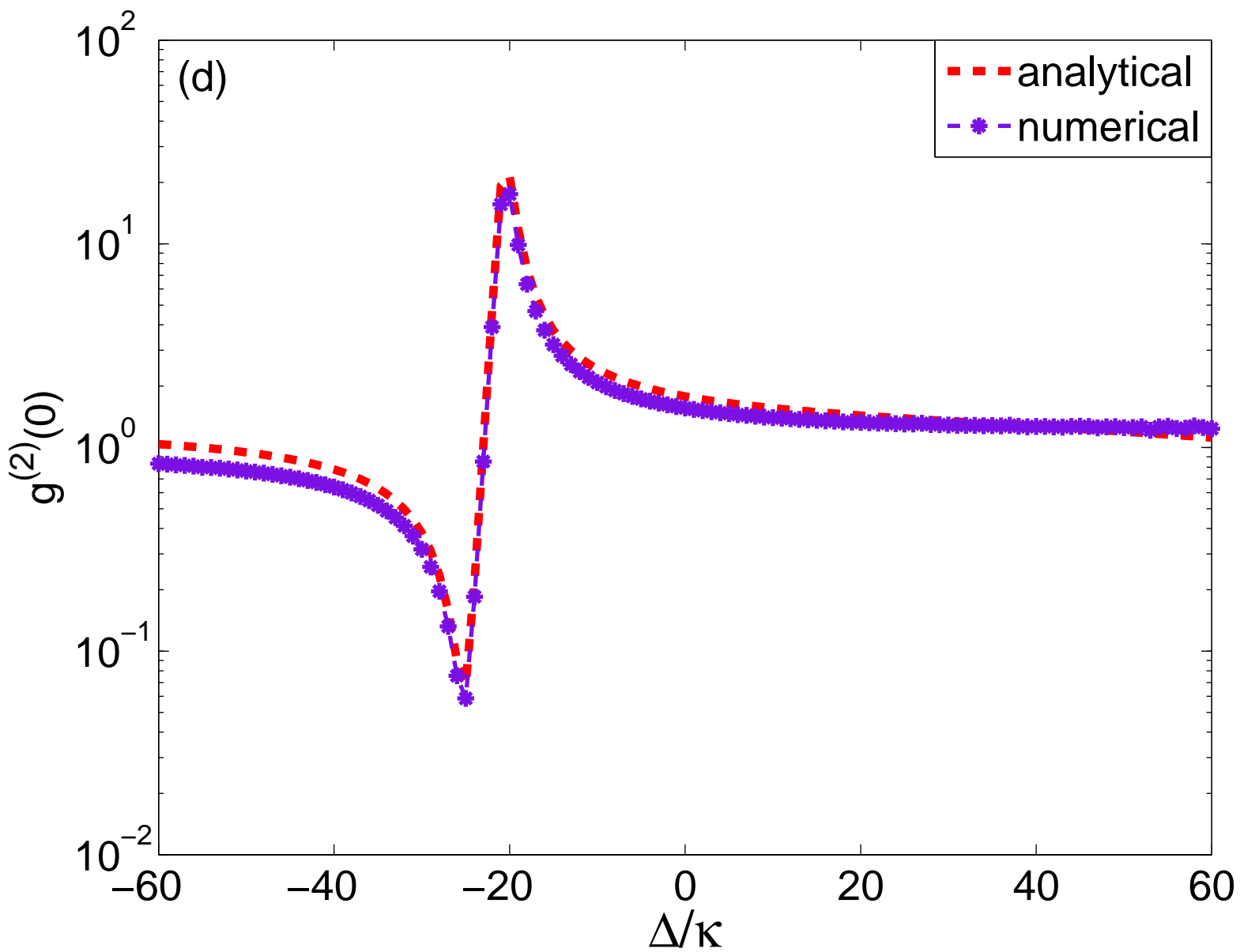
- [1] R. W. Boyd, *Nonlinear Optics* Academic Press, SanDiego, (2008).
- [2] T. C. H. Liew and I. A. Shelykh, *Phys. Rev. A* 80, 161303(R) (2009).
- [3] D. F. Walls and G. J. Milburn, *Quantum Optics* (Springer, Berlin, 1994).
- [4] A. Imamoglu, H. Schmidt, G. Woods, and M. Deutsch *Phys. Rev. L* 79 ,1467 (1997).
- [5] A. D. Wilson-Gordon, V. Bužek, and P. L. Knight, *Phys.Rev. A* 44 ,7647 (1991) .
- [6] F. L. Semião, K. Furuya, G. J. Milburn, *Phys. Rev. A* 79, 063811 (2009)
- [7] M. J. Werner and A. Imamoglu, *Phys. Rev. A* 61, 011801(R) (1999).
- [8] L. Tian and H. J. Carmichael, *Phys. Rev. A* 46 , 6801(R) (1992).
- [9] Y. Wu and L. Deng, *Phys. Rev. Lett.* 93 ,143904 (2004).

- [10] M. J. Hartmann, F. G. S. L. Brandão, and M. B. Plenio, *Nature Phys.* 2, 849 (2006) .
- [11] A. D. Greentree, C. Tahan, J. H. Cole and L. C. L. Hollenberg, *Nature Phys* 2 , 856 (2006).
- [12] A. Ourjoumtsev, A. Kubanek, M. Koch, C. Sames, P.W.H. Pinkse, G. Rempe, K. Murr, *Nature* 474 , 623 (2011).
- [13] B. Dayan et al., *Science* 319,1062 (2008) .
- [14] X. T. Zou and L. Mandel, *Phys. Rev. A* 41, 475 (1990).
- [15] A. J. Hoffman et al., *Phys. Rev. Lett.* 107, 053602 (2011).
- [16] Y-X Liu, X-W Xu, A. Miranowicz, and F. Nori, *Phys. Rev. A* 89, 043818 (2014).
- [17] I. Carusotto et al., *Phys. Rev. Lett.* 103, 033601 (2009).
- [18] M. J. Hartmann, F. G. S. L. Brandao, and M. B. Plenio, *Nature Phys.* 2, 849 (2006).
- [19] D. G. Angelakis, M. F. Santos, and S. Bose, *Phys. Rev. A* 76, 031805 (2007).
- [20] A. Reinhard et al., *Nat. Photonics* 6, 93 (2012).
- [21] Y-M. He et al *Nat. Nanotechnol.* 8, 213 (2013).
- [22] S. Rebic, S. M. Tan, A. S. Parkins, and D. F. Walls, *J. Opt. B*, 1, 490 (1999).
- [23] M. J. Hartmann and M. B. Plenio, *Phys. Rev. Lett.* 99, 103601 (2007).
- [24] P. Rabl, *Phys. Rev. Lett.* 107, 063601 (2011).
- [25] A. Nunnenkamp, K. Børkje, and S. M. Girvin, *Phys. Rev. Lett.* 107, 063602 (2011).
- [26] P. Kómár et al., *Phys. Rev. A* 87, 013839 (2013).
- [27] J-Q Liao and F. Nori ,*Phys. Rev. A* 88, 023853 (2013).

- [28] A. Verger, C. Ciuti, and I. Carusotto, *Phys. Rev. B* 73, 193306 (2006).
- [29] A. Ridolfo, M. Leib, S. Savasta, and M. J. Hartmann, *Phys. Rev. Lett.* 109, 193602 (2012).
- [30] B. Lounis and W. E. Moerner, *Nature* 407, 491 (2000).
- [31] A. Kuzmich et al., *Nature (London)* 423, 731 (2003).
- [32] C. Kurtsiefer, S. Mayer, P. Zarda, and H. Weinfurter, *Phys. Rev. Lett.* 85, 290 (2000).
- [33] A. Faraon et al., *Nature Phys.* 4, 859 (2008).
- [34] X-W Xu and Y. li *Phys. Rev. A* 90, 043822 (2014).
- [35] A. Miranowicz, M. Paprzycka, Y. X. Liu, J. Bajer, and F. Nori, *Phys. Rev. A* 87, 023809 (2013).
- [36] P. Michler et al, *Science* 290, 2282 (2000).
- [37] L. Zhou, L. P. Yang, Y. Li, and C. P. Sun, *Phys. Rev. Lett.* 111, 103604 (2013).
- [38] T. Aoki et al., *Phys. Rev. Lett.* 102, 083601 (2009).
- [39] F.-Y. Hong and S.-J. Xiong, *Phys. Rev. A* 78, 013812 (2008).
- [40] S. Rosenblum, S. Parkins, and B. Dayan, *Phys. Rev. A* 84, 033854 (2011).
- [41] K. M. Birnbaum et al *Nature (London)* 436, 87 (2005).
- [42] A. Majumdar, M. Bajcsy and J. Vučković *Phys. Rev. A.* 85, 041801 (R) (2009).
- [43] E. T. Jaynes and F. W. Cummings, *Proc. IEEE* 51, 89 (1963).
- [44] M. O. Scully and M. suhail zubairy, *Quantum optics* (Cambridge university press, 1997).
- [45] X-W Xu, Y-J Li, Y-X Liu, *Phys. Rev. A* 87, 025803 (2013).
- [46] C. lang et al., *Phys. Rev. lett* 106, 243601 (2011).

- [47] I. Carusotto and C. Ciuti, *Rev. Mod. Phys.*, 85, 299 (2013).
- [48] H. J. Carmichael, R. J. Brecha and P. R. Rice, *Opt. Commun.* 82, 73 (1991).
- [49] S. M. Tan, *J. Opt. B: Quantum Semiclassical Opt.* 1, 424 (1999).
- [50] Schleich W P *Quantum Optics in Phase Space* (Weinheim: Wiley-VCH 2001).
- [51] M. Bienert and G. Morigi, *Phys. Rev. A* 86, 053402 (2012).
- [52] S. Ferretti and D. Gerace, *Phys. Rev. B* 85, 033303 (2012).
- [53] S. Weis et al., *Science* 330, 1520 (2010).
- [54] M. D. Lukin, *Rev. Mod. Phys.* 75, 457 (2003).
- [55] M. Koch et al., *Phys. Rev. Lett.* 107, 023601(2011).
- [56] S. Ferretti et al., *Phys. Rev. A* 82, 013841 (2010).
- [57] R. J. Brecha, P. R. Rice, and M. Xiao, *Phys. Rev. A* 59, 2392 (1999).
- [58] C. Gardiner and P. Zoller, *Quantum Noise* (Springer, Berlin, 2004).
- [59] O. Kyriienko, I. A. Shelykh, and T. C. H. Liew, *Phys. Rev. A* 90, 033807 (2014).
- [60] H. Z. Shen, Y. H. Zhou, and X. X. Yi , *Phys. Rev. A* 90, 023849 (2014).
- [61] A. Faraon, A. Majumdar and J. Vučković *Phys. Rev. A.* 81, 033838 (2010).
- [62] Leibfried D, Meekhof D M, King B E, Monroe C, Itano W M and Wineland D J *Phys. Rev. Lett.* 77, 4281 (1996).
- [63] Blatt R and Roos C F *Nature Phys.* 8 277 (2012).
- [64] J. Z Bernád, H. Frydrych and G .Alber *J. Phys. B: At. Mol. Opt. Phys.* 46 , 235501 (2013).
- [65] A. D. Boozer, A. Boca, R. Miller, T. E. Northup, and H. J. Kimble, *Phys. Rev. Lett.* 97, 083602 (2006).

- [66] T. Kampschulte et al, Phys. Rev. Lett. 105, 153603 (2010).
- [67] D. R. Leibrandt, J. Labaziewicz, V. Vuletić, and I. L. Chuang, Phys. Rev. Lett. 103, 103001 (2009).



0

Δ/κ

